Performance of CUF approach to analyze the structural behavior of slender bodies

Performance of CUF Approach to Analyze the Structural Behavior of Slender Bodies

Erasmo Carrera[1]; Marco Petrolo[2]; and Enrico Zappino[3]

Introduction

Beam theories are extensively used to analyze the structural behavior of slender bodies, such as columns, arches, blades, aircraft wings, and bridges. The main advantage of beam models is that they reduce the problems in a set of variables that depend only on the beam-axis coordinate. The one-dimensional (1D) structure elements obtained are simpler and computationally more efficient than two-dimensional (2D) (plate/shell) and three-dimensional (3D) (solid) elements. This feature means that beam theories are still very attractive for the static and dynamic analysis of structures.

The classical, most employed theories are those by Euler-Bernoulli (Euler 1744), de Saint-Venant (1856), and Timoshenko 1921)). The first two do not account for transverse shear deformations. Timoshenko foresees a uniform shear distribution along the cross section of the beam. Mucichescu (1984) made a comparison between Eulero-Bernoulli and Timoshenko. None of these are able to detect nonclassical effects such as warping, out- and in-plane deformations, torsion-bending coupling, and localized boundary conditions (BCs), both geometrical and mechanical. These kinds of effects are usually the result of small slenderness ratios, thin-walled structures, and the anisotropy of the materials.

Many attempts have been proposed to overcome the limitations of classical theories and to permit the application of 1D models to any beam geometries subjected to any boundary conditions. Examples of these models can be found in many well-known books on the theory of elasticity (e.g., Novozhilov 1961).

In a recent development, beam models have been obtained by means of different approaches; namely, introduction of shear correction factors, use of warping functions based on de Saint-Venat's solution, variational asymptotic solution (VABS), general-ized beam theories (GBT), and higher-order beam models. Some of the most relevant contributions are discussed subsequently.

A considerable amount of work has been done to try to improve the global response of classical beam theories by the use of appropriate shear correction factors, as in the books by Timoshenko and Goodier (1970) and by Sokolnikoff (1956). Among the many available articles, the papers by Cowper (1966), Krishna Murthy (1985), Pai and Schulz (1999), and Mechab et al. (2008) are of particular interest. An extensive effort was made by Gruttmann et al. (1999) and Gruttman and Wagner (2001; Wagner and Gruttmann 2002) t o compute shear correction factors, and many structural types were considered, including torsional and flexural shearing stresses in prismatic beams, arbitrary shaped cross sections, wide, thin-walled structures, and bridge-like structures.

El Fatmi (2007a, b) introduced an improvement of the displacement models over the beam section by introducing a warping function ϕ to improve the description of normal and shear stress of the beam. By means of this model, end effects as a result of boundary conditions were investigated, as in the work by Krayterman and Krayterman (1987). The de Saint-Venant solution has been the theoretical base of many advanced beam models. The 3D elasticity equations were reduced to beam-like structures by Ladevéze and Simmonds (1998). The resulting solution was modeled as the sum of a de Saint-Venant part and a residual part and applied to

[2]Research Scientist, Dept. of Mechanical and Aerospace Engineering, Politecnico di Torino, Corso Duca degli Abruzzi 24, 10129 Torino, Italy; formerly, Ph.D. Candidate, Dept. of Mechanical and Aerospace Engineering, Politecnico di Torino, and Institut Jean Le Rond d'Alembert, Paris, France. E-mail: marco.petrolo@polito.it

[3]Ph.D. Candidate, Dept. of Mechanical and Aerospace Engineering, Politecnico di Torino, Corso Duca degli Abruzzi 24, 10129 Torino, Italy. E-mail: enrico.zappino@polito.it

[1]Professor of Aerospace Structures and Computational Aeroelasticity, Dept. of Mechanical and Aerospace Engineering, Politecnico di Torino, Corso Duca degli Abruzzi 24, 10129 Torino, Italy (corresponding author). E-mail: erasmo.carrera@polito.it

high aspect ratio beams with thin-walled sections. Further beam theories were based on the displacements field proposed by Ieşan (1986) and solved by means of a semi-analytical finite element by Dong et al. (2001).

Asymptotic type expansion in conjunction with variational methods has been proposed by Berdichevsky et al. (1992), in which a commendable review of previous works on beam theory development is given. This work has been the origin of an alternative approach to constructing refined beam theories. A characteristic parameter (e.g., the cross-section thickness for a beam) is exploited to build an asymptotic series. Those terms that exhibit the same order of magnitude as the parameter when it vanishes are retained. Some valuable contributions are those by Volovoi and Hodges (2000), Yu et al. (2002), and Yu and Hodges (2004).

Generalized beam theories originated with Schardt's work (1966, 1989). GBT improves classical theories by using piece-wise beam descriptions of thin-wall sections. It has been extensively employed and extended in various forms by Silvetre et al. (Silvestre and Camotim 2002; Silvestre 2007).

A review was made by Kapania and Raciti (1989), focusing on: bending, vibration, wave propagations, buckling, and post-buckling. Aeroelastic problems of thin-walled beams were considered in the articles by Librescu and Song (1992) and Qin and Librescu (2002).

Many other higher-order theories have been introduced to include nonclassical effects that are based on enhanced displacement fields over the beam cross section. Some considerations on higher-order beam elements were made by Washizu (1968). An advanced model was proposed by Kanok-Nukulchai and Shik Shin (1984); they improved classical finite beam elements that introduced new degrees of freedom to describe cross-section behavior. The previous literature overview clearly shows the interest in further developments on refined theories for beams.

The present work is focused on refined theories with only generalized displacement variables for the static analysis of compact and thin-walled, bridge-like sections. Higher-order models are obtained in the framework of the Carrera Unified Formulation (CUF). This formulation has been developed over the last decade for plate/shell models (Carrera 1995, 2002, 2003; Carrera et al. 2008), and it has recently been extended to beam modelings (Carrera and Giunta 2010). The present beam formulation has been exploited for the static analyses of compact and thin-walled structures (Carrera et al. 2010a). Free-vibration analyses have been carried out on hollow cylindrical and wing models (Carrera et al. 2011, 2012). A beam model with only displacement degrees of freedom has been developed (Carrera and Petrolo 2011, 2012); it has been concluded that full displacement models are required to accurately analyze beams with arbitrary sections subjected to combined bending and/or torsion loadings.

CUF is a hierarchical formulation that considers the order of the model as a free-parameter (i.e., as input) of the analysis; in other words, refined models are obtained with no need for ad hoc formulations. Beam theories are obtained on the basis of Taylor-type expansions. Euler-Bernoulli and Timoshenko beam theories are obtained as particular cases. The finite-element method is used to handle arbitrary geometries and geometrical and loading conditions. This work is not intended to propose new finite elements but to propose new higher-order structural models. The finite-element formulation is used as a tool to test the validity of the proposed models for a large number of geometrical and mechanical boundary conditions (BCs) layouts. The FEM approach adopted is a classical one, and it was preferred to closed-form solutions to carry out analyses on arbitrary structural configurations. The present paper considers the accurate evaluation of stress fields in three different beam configurations: square, C-shaped, and bridge-like sections. Bending, torsion, and end-effects analyses have been conducted and displacement and stress fields have been evaluated. The results are compared with analytical models, 3D finite elements, and data retrieved from literature. Isotropic and orthotropic materials have been used. Shear correction factors related to various beam models are compared.

The paper is organized as follows: Brief descriptions of the adopted beam theories and the finite element formulation are given in the first section; after that, the structural problems addressed, together with the results and discussion, are provided; the main conclusions are then outlined in the last section.

Advanced Beam Models and Related FE Formulations

The adopted coordinate frame is presented in Fig. 1. The beam boundaries over y are $0 \leq y \leq L$. The displacement vector is:

$$\mathbf{u}(x,y,z) = \{\, u_x \quad u_y \quad u_z \,\}^T \tag{1}$$

The superscript T represents the transposition operator. Stress, $\boldsymbol{\sigma}$, and strain, $\boldsymbol{\epsilon}$, components are grouped as follows:

$$\begin{aligned} \boldsymbol{\sigma}_p &= \{\, \sigma_{zz} \quad \sigma_{xx} \quad \sigma_{zx} \,\}^T, \qquad \boldsymbol{\epsilon}_p = \{\, \epsilon_{zz} \quad \epsilon_{xx} \quad \epsilon_{zx} \,\}^T \\ \boldsymbol{\sigma}_n &= \{\, \sigma_{zy} \quad \sigma_{xy} \quad \sigma_{yy} \,\}^T, \qquad \boldsymbol{\epsilon}_n = \{\, \epsilon_{zy} \quad \epsilon_{xy} \quad \epsilon_{yy} \,\}^T \end{aligned} \tag{2}$$

The subscript n stands for terms lying on the cross section, whereas p stands for terms lying on planes that are orthogonal to Ω. Linear strain-displacement relations are used as follows:

$$\boldsymbol{\epsilon}_p = \boldsymbol{D}_p \mathbf{u} \qquad \boldsymbol{\epsilon}_n = \boldsymbol{D}_n \mathbf{u} = (\boldsymbol{D}_{n\Omega} + \boldsymbol{D}_{ny})\mathbf{u} \tag{3}$$

with

$$\boldsymbol{D}_p = \begin{bmatrix} 0 & 0 & \frac{\partial}{\partial z} \\ \frac{\partial}{\partial x} & 0 & 0 \\ \frac{\partial}{\partial z} & 0 & \frac{\partial}{\partial x} \end{bmatrix}, \qquad \boldsymbol{D}_{n\Omega} = \begin{bmatrix} 0 & \frac{\partial}{\partial z} & 0 \\ 0 & \frac{\partial}{\partial x} & 0 \\ 0 & 0 & 0 \end{bmatrix},$$
$$\boldsymbol{D}_{ny} = \begin{bmatrix} 0 & 0 & \frac{\partial}{\partial y} \\ \frac{\partial}{\partial y} & 0 & 0 \\ 0 & \frac{\partial}{\partial y} & 0 \end{bmatrix} \tag{4}$$

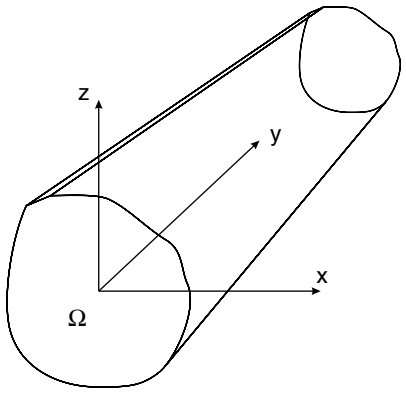

Fig. 1. Coordinate frame of the beam model

The Hooke law is exploited as

$$\boldsymbol{\sigma} = \boldsymbol{C}\boldsymbol{\epsilon} \tag{5}$$

According to Eq. (2), the previous equation becomes

$$\boldsymbol{\sigma}_p = \tilde{\boldsymbol{C}}_{pp}\boldsymbol{\epsilon}_p + \tilde{\boldsymbol{C}}_{pn}\boldsymbol{\epsilon}_n \qquad \boldsymbol{\sigma}_n = \tilde{\boldsymbol{C}}_{np}\boldsymbol{\epsilon}_p + \tilde{\boldsymbol{C}}_{nn}\boldsymbol{\epsilon}_n \tag{6}$$

In the case of isotropic material, the matrices $\tilde{\boldsymbol{C}}_{pp}$, $\tilde{\boldsymbol{C}}_{nn}$, $\tilde{\boldsymbol{C}}_{pn}$, and $\tilde{\boldsymbol{C}}_{np}$ are

$$\tilde{\boldsymbol{C}}_{pp} = \begin{bmatrix} \tilde{C}_{11} & \tilde{C}_{12} & 0 \\ \tilde{C}_{12} & \tilde{C}_{22} & 0 \\ 0 & 0 & \tilde{C}_{66} \end{bmatrix}, \qquad \tilde{\boldsymbol{C}}_{nn} = \begin{bmatrix} \tilde{C}_{55} & 0 & 0 \\ 0 & \tilde{C}_{44} & 0 \\ 0 & 0 & \tilde{C}_{33} \end{bmatrix},$$
$$\tilde{\boldsymbol{C}}_{pn} = \tilde{\boldsymbol{C}}_{np}^T = \begin{bmatrix} 0 & 0 & \tilde{C}_{13} \\ 0 & 0 & \tilde{C}_{23} \\ 0 & 0 & 0 \end{bmatrix} \tag{7}$$

For the sake of brevity, the dependence of coefficients $[\tilde{C}]_{ij}$ versus the Young's modulus and Poisson's ratio and the formulation for orthotropic materials are not reported in this paper. It can be found in the books by Tsai (1988) and Reddy (2004).

In the framework of the CUF (Carrera 2002, 2003; Carrera and Giunta 2010; Carrera et al. 2010a, b; Carrera and Petrolo 2011), the displacement field is assumed as an expansion in terms of generic functions, F_τ as follows:

$$\mathbf{u} = F_\tau(x,z)\mathbf{u}_\tau(y), \qquad \tau = 1,2,\ldots,M \tag{8}$$

where F_τ = functions of coordinates x and z on the cross section; $\mathbf{u}_\tau$ = displacement vector; and M = number of terms of the expansion of order N. According to the Einstein notation, the repeated subscript τ indicates summation. Eq. (8) consists of a Maclaurin expansion that uses as the base the 2D polynomials $x^i z^j$, where i and j are positive integers. A generic N-order displacement field is given by

$$\begin{aligned} u_x &= \sum_{N_i=0}^{N}\left[\sum_{M=0}^{N_i} x^{N-M}z^M u_{x_{\frac{N(N+1)+M+1}{2}}}\right] \\ u_y &= \sum_{N_i=0}^{N}\left[\sum_{M=0}^{N_i} x^{N-M}z^M u_{y_{\frac{N(N+1)+M+1}{2}}}\right] \\ u_z &= \sum_{N_i=0}^{N}\left[\sum_{M=0}^{N_i} x^{N-M}z^M u_{z_{\frac{N(N+1)+M+1}{2}}}\right] \end{aligned} \tag{9}$$

For example, the second-order displacement field is

$$\begin{aligned} u_x &= u_{x_1} + xu_{x_2} + zu_{x_3} + x^2u_{x_4} + xzu_{x_5} + z^2u_{x_6} \\ u_y &= u_{y_1} + xu_{y_2} + zu_{y_3} + x^2u_{y_4} + xzu_{y_5} + z^2u_{y_6} \\ u_z &= u_{z_1} + xu_{z_2} + zu_{z_3} + x^2u_{z_4} + xzu_{z_5} + z^2u_{z_6} \end{aligned} \tag{10}$$

where u_{x_τ}, u_{y_τ} and u_{z_τ} are y-dependent. The Timoshenko beam model (TBM) can be obtained by acting on the F_τ expansion. Two conditions must be imposed. The first is a first-order approximation kinematic field:

$$\begin{aligned} u_x &= u_{x_1} + xu_{x_2} + zu_{x_3} \qquad u_y = u_{y_1} + xu_{y_2} + zu_{y_3} \\ u_z &= u_{z_1} + xu_{z_2} + zu_{z_3} \end{aligned} \tag{11}$$

Second, the displacement components u_x and u_z must be constant above the cross section:

$$u_{x_2} = u_{z_2} = u_{x_3} = u_{z_3} = 0 \tag{12}$$

The Euler-Bernoulli beam model (EBBM) can be obtained through the penalization of ϵ_{xy} and ϵ_{zy}. This condition can be imposed by using a penalty value χ in the following constitutive equations:

$$\sigma_{xy} = \chi\tilde{C}_{55}\epsilon_{xy} + \chi\tilde{C}_{45}\epsilon_{zy} \qquad \sigma_{zy} = \chi\tilde{C}_{45}\epsilon_{xy} + \chi\tilde{C}_{44}\epsilon_{zy} \tag{13}$$

Classical theories and first-order models require the assumption of opportunely reduced material stiffness coefficients to correct Poisson's locking [see Carrera and Brischetto (2008)]. Unless differently specified, for classical and first-order models, Poisson's locking is corrected according to Carrera and Giunta (2010).

Introducing the shape functions, N_i, and the nodal displacement vector, $\mathbf{q}_{\tau i}$ as

$$\mathbf{q}_{\tau i} = \{\, q_{u_{x_{\tau i}}} \quad q_{u_{y_{\tau i}}} \quad q_{u_{z_{\tau i}}} \,\}^T \tag{14}$$

the displacement vector becomes

$$\mathbf{u}(x,y,z) = N_i(y)F_\tau(x,z)\mathbf{q}_{\tau i}, \qquad i = 1,2,\ldots,K \tag{15}$$

where K = number of the nodes on the element. For the sake of brevity, the shape functions, N_i, are not reported here. They can be found in many books; for instance, in Bathe (1996). Elements with four nodes (B4) are herein formulated; that is, a cubic approximation along the y axis is adopted. It has to be highlighted that, although the order of the beam model, N, is related to the expansion on the cross section, the number of nodes per each element, K, is related to the approximation along the longitudinal axis. These two parameters are totally free and not related to each other. An N-order beam model is, therefore, a theory that exploits an N-order polynomial to describe the kinematics of the cross section. The stiffness matrix of the elements and the external loadings, which are consistent with the model, are obtained by means of the principle of virtual displacements as follows:

$$\delta L_{\text{int}} = \int_V (\delta\boldsymbol{\epsilon}_p^T\boldsymbol{\sigma}_p + \delta\boldsymbol{\epsilon}_n^T\boldsymbol{\sigma}_n)dV = \delta L_{\text{ext}} \tag{16}$$

where L_{int} = strain energy; L_{ext} = work of the external loadings; and δ = virtual variation. The virtual variation of the strain energy is rewritten using Eqs. (3), (6), and (15); in a compact format it becomes

$$\delta L_{\text{int}} = \delta\mathbf{q}_{\tau i}^T\mathbf{K}^{ij\tau s}\mathbf{q}_{sj} \tag{17}$$

where $\mathbf{K}^{ij\tau s}$ = stiffness matrix in the form of the fundamental nucleus. Its components are

$$
\begin{aligned}
K_{xx}^{ij\tau s} &= \tilde{C}_{22}\int_\Omega F_{\tau,x}F_{s,x}d\Omega\int_l N_iN_jdy + \tilde{C}_{66}\int_\Omega F_{\tau,z}F_{s,z}d\Omega\int_l N_iN_jdy + \tilde{C}_{44}\int_\Omega F_\tau F_s d\Omega\int_l N_{i,y}N_{j,y}dy\\
K_{xy}^{ij\tau s} &= \tilde{C}_{23}\int_\Omega F_{\tau,x}F_s d\Omega\int_l N_iN_{j,y}dy + \tilde{C}_{44}\int_\Omega F_\tau F_{s,x}d\Omega\int_l N_{i,y}N_j dy\\
K_{xz}^{ij\tau s} &= \tilde{C}_{12}\int_\Omega F_{\tau,x}F_{s,z}d\Omega\int_l N_iN_jdy + \tilde{C}_{66}\int_\Omega F_{\tau,z}F_{s,x}d\Omega\int_l N_iN_j dy\\
K_{yx}^{ij\tau s} &= \tilde{C}_{44}\int_\Omega F_{\tau,x}F_s d\Omega\int_l N_iN_{j,y}dy + \tilde{C}_{23}\int_\Omega F_\tau F_{s,x}d\Omega\int_l N_{i,y}N_j dy\\
K_{yy}^{ij\tau s} &= \tilde{C}_{55}\int_\Omega F_{\tau,z}F_{s,z}d\Omega\int_l N_iN_jdy + \tilde{C}_{44}\int_\Omega F_{\tau,x}F_{s,x}d\Omega\int_l N_iN_jdy + \tilde{C}_{33}\int_\Omega F_\tau F_s d\Omega\int_l N_{i,y}N_{j,y}dy\\
K_{yz}^{ij\tau s} &= \tilde{C}_{55}\int_\Omega F_{\tau,z}F_s d\Omega\int_l N_iN_{j,y}dy + \tilde{C}_{13}\int_\Omega F_\tau F_{s,z}d\Omega\int_l N_{i,y}N_j dy\\
K_{zx}^{ij\tau s} &= \tilde{C}_{12}\int_\Omega F_{\tau,z}F_{s,x}d\Omega\int_l N_iN_jdy + \tilde{C}_{66}\int_\Omega F_{\tau,x}F_{s,z}d\Omega\int_l N_iN_j dy\\
K_{zy}^{ij\tau s} &= \tilde{C}_{13}\int_\Omega F_{\tau,z}F_s d\Omega\int_l N_iN_{j,y}dy + \tilde{C}_{55}\int_\Omega F_\tau F_{s,z}d\Omega\int_l N_{i,y}N_j dy\\
K_{zz}^{ij\tau s} &= \tilde{C}_{11}\int_\Omega F_{\tau,z}F_{s,z}d\Omega\int_l N_iN_jdy + \tilde{C}_{66}\int_\Omega F_{\tau,x}F_{s,x}d\Omega\int_l N_iN_jdy + \tilde{C}_{55}\int_\Omega F_\tau F_s d\Omega\int_l N_{i,y}N_{j,y}dy
\end{aligned}
\tag{18}
$$

It should be noted that no assumptions on the approximation order have been done. It is, therefore, possible to obtain refined beam models without changing the formal expression of the nucleus components. This is the key point of CUF, which permits, with only nine FORTRAN statements, to implement any-order beam theories. The shear locking is corrected through the selective integration [see Bathe (1996)].

Numerical Analysis and Discussion

The static analysis of different beam models is conducted in this section. The preliminary analyses are devoted to convergence studies and are conducted on a simply supported compact section made of aluminium. Two comparisons with results from literature are given; the first on the end effects of a cantilevered beam and the second on a thin-walled section analysis. The rest of the work is devoted to the investigation of the structural behavior of a bridge-like beam made of steel. If not differently stated, cubical elements (B4) are used in the axial discretization; the nodes are uniformly distributed along the longitudinal axis. Each node presents $M \times 3$ degrees of freedom, where M = number of terms of the N-order expansion on the cross section.

Simply Supported Compact Section

A simply supported square beam is considered as a preliminary assessment of the present beam model. Further results with different geometries and boundary conditions have been presented in Carrera et al. (2010a). The geometry of the section is shown in Fig. 2. Two length-to-thickness ratios, L/h, of 100 and 10 are considered . Therefore, thin and moderately thick structures are considered. The cross-section edge dimensions, b and h, are equal to 0.1 m. Young's modulus, E, is equal to 75 GPa. The Poisson's ratio, ν, is equal to 0.33. A concentrated load, P_z, is applied at 0, $L/2$, 0, and is equal to 50 N. A benchmark solution is obtained by means of the Euler-Bernoulli beam theory as follows:

$$u_{z_b} = \frac{1}{48}\frac{P_z L^3}{EI} \tag{19}$$

where I = moment of inertia of the cross section. Tables 1 and 2 show the vertical displacement, u_z, at the loading point for different

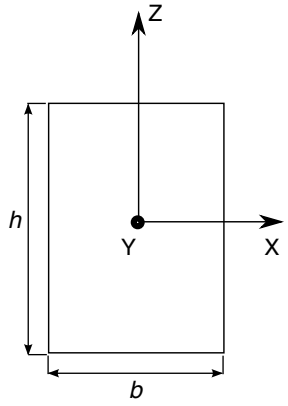

Fig. 2. Rectangular cross section

Table 1. Vertical Displacements for Different Beam Theories and Meshes

Number of elements	EBBM	TBM	$N = 1$	$N = 2$
	$u_z \times 10^3$ (m), $u_{z_b} \times 10^3 = 1.667$ (m)			
2	1.667	1.667	1.667	1.667
6	1.667	1.667	1.667	1.667
10	1.667	1.667	1.667	1.667
40	1.667	1.667	1.667	1.667

Note: $L/h = 100$; simply supported compact beam loaded with a concentrated load.

Table 2. Vertical Displacements for Different Beam Theories and Meshes

Number of elements	EBBM	TBM	$N = 1$	$N = 2$	$N = 3$	$N = 4$
$u_z \times 10^6$ (m), $u_{z_b} \times 10^6 = 1.667$ (m)						
2	1.667	1.712	1.712	1.712	1.719	1.720
6	1.667	1.712	1.712	1.712	1.720	1.722
10	1.667	1.712	1.712	1.713	1.720	1.723
40	1.667	1.712	1.712	1.713	1.720	1.724

Note: $L/h = 10$; simply supported compact beam loaded with a concentrated load.

beam theories, meshes, and length-to-thickness ratios. B4 elements are used. The following considerations hold:

1. Two B4 elements are enough to obtain convergence for the case of a slender beam, whereas 40 cubic elements are needed for $L/h = 10$.
2. As far as the theory order is concerned, a slender beam requires a second-order model ($N = 2$) to detect the vertical displacement. The effects of the cubic and fourth-order terms are appreciable in the case of a moderately thick beam.
3. The EBBM is able to furnish the same result as the refined theories for $L/h = 100$. As the thickness increases, the differences between classical theories and higher-order ones also increase.
4. The TBM and the linear model ($N = 1$) furnish a larger value of u_y than the EBBM for $L/h = 10$. This means that shear effects play a role in the mechanical response of a moderately thick beam, whereas the effect of the linear terms of the in-plane displacement components is negligible.

The 40 B4 element mesh will be used for all the following analyses because it offers good accuracy. The second assessment of the proposed model concerns a comparison with an analytical Navier-type solution. The analytical results are taken from Carrera and Giunta (2010). A rectangular cross section is considered with $h/b = 100$. Two different length-to-thickness ratios (100 and 10) are adopted. A distributed sinusoidal load, $p_z(y)$, is applied to the top surface, $z = h/2$, and its expression is

$$p_z(y) = P_{zz} \sin\left(\frac{\pi y}{L}\right) \tag{20}$$

Three stress components are considered: σ_{yy} and σ_{zz} at [0, 0, $h/2$] and σ_{yz} at [0, 0, 0]. Tables 3 and 4 present the results of the considered L/h values. Excellent agreement is generally found. It should be pointed out that the detection of σ_{zz} requires at least a second-order beam theory.

End-Effects on Compact Sections

A cantilevered beam is analyzed to investigate the end effects caused by the boundary conditions. A rectangular compact section is considered. The geometry is shown in Fig. 2; the height h is assumed to be equal to 1 m; the ratio b/h is assumed to be equal to 0.5; and the aspect ratio L/h is assumed to be six, where L is the length of the beam. Two loading settings are considered: a concentrated load in the z-direction, F_z, and a concentrated load in the y-direction, F_y. Both loads are posed in [0, L, 0] and are equal to 1 N. An orthotropic material is considered; its features are shown in Table 5. A total of 40 B4 elements are used in the axial discretization. A comparison with higher-order beam models (Ghazouani and El Fatmi 2010) and a 3D FEM solution is given. Fig. 3(a) shows the value of the normal tension σ_{yy} in the area close to the constraint for a beam subject to bending load. The diagram shows the following conclusions:

1. The classical theory, EBBM, does not predict the local effects due to the boundary conditions.
2. The end-effects on σ_{yy} are confined to an area of length equal to three times the height, h, of the cross section.
3. The results from a third-order beam model agree with those from literature.
4. At the constrained cross section, the role of higher-order models is extremely evident. An $N = 5$ model is able to increase the accuracy of the model significantly. The adoption of higher-order CUF beam models is able to improve the solution from other models and leads to the 3D solution for increasing beam orders.

In Fig. 3(b), a traction load is considered. The results are given in terms of $(\sigma_t)/(\sigma_{yy}^{SV})$, where σ_t is equal to $(\sigma_{xx} + \sigma_{zz})/2$ and σ_{yy}^{SV}

Table 3. Comparison of Various Stress Components Obtained by Using an Analytical Model and the Present Beam Formulation

Model	EBBM	TBM	$N = 1$	$N = 2$	$N = 3$	$N = 4$
σ_{yy}[a]						
Carrera and Giunta (2010)	1.000	1.000	1.000	1.000	1.000	1.000
Present beam	1.000	1.000	1.000	1.000	1.000	1.000
σ_{zz}[a]						
Carrera and Giunta (2010)	—[b]	—	0.524	1.012	1.233	1.000
Present beam	—	—	3,507.8	1.012	1.233	1.000
σ_{yz}[a]						
Carrera and Giunta (2010)	—	0.667	0.667	0.705	1.000	1.000
Present beam	—	0.667	0.667	0.706	1.000	1.000

Note: $L/h = 100$; simply supported beam loaded with a distributed sinusoidal load.
[a]$\sigma_{yy} = (\pi^2/6)(h^2/L^2)(\sigma_{yy}/P_z)$; $\sigma_{zz} = \sigma_{zz}/P_z$; $\sigma_{yz} = (2\pi/3)(h/L)(\sigma_{yz}/P_z)$.
[b]Result not provided by the theory.

Table 4. Comparison of Various Stress Components Obtained Via an Analytical Model and the Present Beam Formulation

Model	EBBM	TBM	$N = 1$	$N = 2$	$N = 3$	$N = 4$
σ_{yy}[a]						
Carrera and Giunta (2010)	1.000	1.000	0.996	1.000	1.005	1.003
Present beam	1.000	1.000	0.998	0.998	1.004	1.002
σ_{zz}[a]						
Carrera and Giunta (2010)	—[b]	—	0.522	1.014	1.233	1.000
Present beam	—	—	35.6	1.014	1.233	1.000
σ_{yz}[a]						
Carrera and Giunta (2010)	—	0.667	0.667	0.704	0.999	0.999
Present beam	—	0.667	0.667	0.704	0.999	0.999

Note: $L/h = 10$; simply supported beam loaded with a distributed sinusoidal load.
[a]$\sigma_{yy} = (\pi^2/6)(h^2/L^2)(\sigma_{yy}/P_z)$; $\sigma_{zz} = \sigma_{zz}/P_z$; $\sigma_{yz} = (2\pi/3)(h/L)(\sigma_{yz}/P_z)$.
[b]Result not provided by the theory.

Table 5. Mechanical Properties of the Orthotropic Material

Material property	Value
E_{11} [GPa]	206.80
E_{22} [GPa]	5.17
E_{33} [GPa]	5.17
G_{12} [GPa]	3.10
G_{13} [GPa]	3.10
G_{23} [GPa]	2.55
ν_{12}	0.25
ν_{13}	0.25
ν_{23}	0.25

is equal to the force F_y divided by the area of the cross section. It is possible to highlight the conclusions as follows:

1. The end-effects on σ_t are confined to an area of length equal to the height, h, of the cross section.
2. The first-order beam model results match those from literature.
3. The results from a third-order beam model agree with those from a 3D FEM analysis.

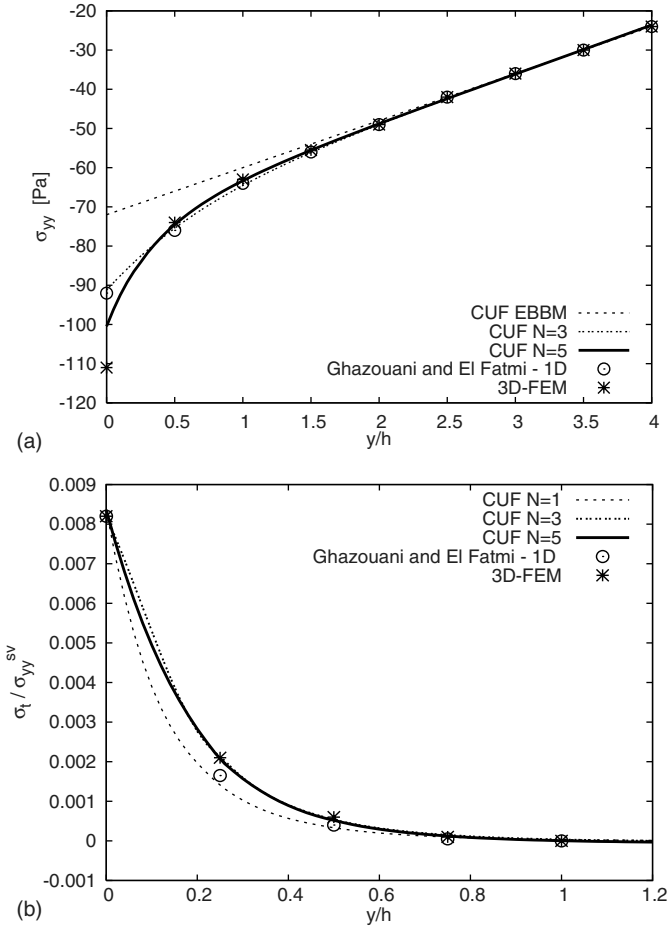

Fig. 3. End effects caused by the boundary conditions on a cantilevered beam with rectangular compact section; comparison of the results from CUF beam theories and those from Ghazouani and El Fatmi (2010): (a) bending loading and stresses evaluated in $x = 0$ and $z = h/2$; (b) traction loading and stresses evaluated in $x = 0$ and $z = 0$; $\sigma_t = (\sigma_{zz} + \sigma_{xx})/2$

C-Shaped Thin-Walled Section

A cantilevered C-shaped cross-section beam is considered to evaluate the capabilities of the present beam model in the thin-walled structures analysis. The geometric characteristics have been taken from Vlasov (1961). Fig. 4 shows the cross-section geometry; the height h is considered equal to 5 m; b is equal to 3.5 m; the thickness, t, is assumed to be 0.2 m; and the length of the beam, L, is 18 m. Young's modulus, E, is equal to 30 GPa, and the Poisson ratio, ν, is equal to 0.33. Two forces, $F^x{}_1$ and $F^x{}_2$ (see Fig. 4), equal to 200 kN, are posed in $[1.095, \pm h/2, L]$, acting in the $\pm x$-direction to reproduce an equivalent torsional moment, $M_{t_{eq}}$, equal to 1,000 kNm. A total of 10 elements B4 are used in the axial discretization.

The twisting angle, Θ, is used to give comparisons with results from solid elements analysis and from literature (Vlasov 1961; Tralli 1986; Back and Will 1998; Kim and Kim 2005; E l Fatmi 2007c).

In the classical models, on the basis of the displacements' degree of freedom, Θ may be defined as

$$\tan(\Theta) = \frac{\partial u_x}{\partial z} = \frac{\partial u_z}{\partial x}$$

Considering Eq. (10), the twisting angle in the CUF formulation can be written as

$$\tan(\Theta_x) = \frac{\partial u_x}{\partial z} = u_{x_2} + x u_{x_5} + 2z u_{x_6} + \cdots$$

$$\tan(\Theta_z) = \frac{\partial u_z}{\partial x} = u_{z_3} + 2x u_{z_4} + z u_{z_5} + \cdots$$

This equation shows that the twisting angle is not a property of the whole section but a property of the point; also, the equivalence $\partial u_x/\partial z = \partial u_z/\partial x$ is not automatically satisfied. To compare the results with those from literature in this work only, the constant term is considered in the evaluation of the twisting angle so that θ has been defined as

$$\Theta = \frac{\arctan(u_{x_2}) + \arctan(u_{z_3})}{2}$$

Table 6 shows the value of the twisting angle in many points along the y-axis and for various structural models. Fig. 5 shows the deformed cross section at beam tip evaluated by means of a different structural model; the displacements have been scaled by a $\times 100$ factor to make the figure clearer. Fig. 6 reports the twisting angle

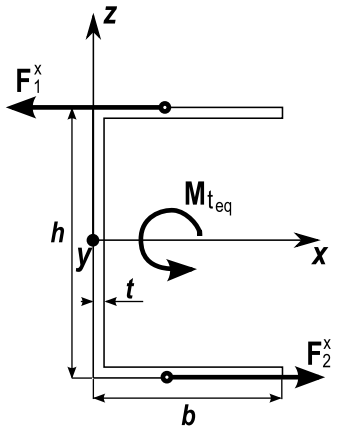

Fig. 4. C-shaped cross-section geometry and loading

Table 6. Twisting Angle (Θ) Along the y-Axis of a Beam with C-shaped Cross Section under Torsional Loading—Comparison of Various 1D and Solid Models

		y (m)					
		3	6	9	12	15	18
Model	DOFs	Θ(rad) $\times 10^{-3}$					
Vlasov (1961)		0.163	0.611	1.284	2.124	3.075	4.081
Tralli (1986)		0.193	0.669	1.369	2.234	3.209	4.239
Back and Will (1998)		0.188	0.659	1.354	2.215	3.185	4.210
Kim and Kim (2005) (CASE 4)		0.193	0.669	1.368	2.233	3.207	4.236
El Fatmi (2007c)		—	—	—	—	—	4.203
CUF $N = 4$	1,395	0.136	0.444	0.875	1.392	1.970	2.708
CUF $N = 6$	2,604	0.115	0.531	1.163	1.963	2.939	4.268
CUF $N = 10$	6,138	0.192	0.723	1.541	2.573	3.777	5.136
Nastran	22,200	0.229	0.785	1.603	2.618	3.704	4.966

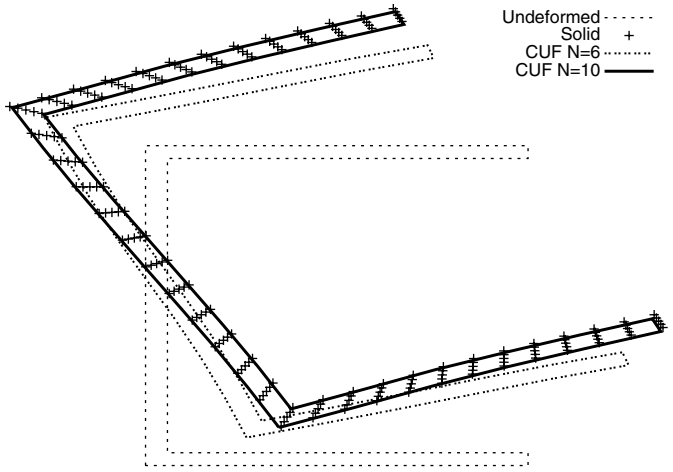

Fig. 5. Deformation of C-shaped cross-section beam at $y = L$ for different structural models; displacements amplification $\times$ 100

behavior along the y-axis evaluated by means of different structural models.

The following considerations hold:

1. A tenth-order beam model is needed to reach a good level of accuracy in the evaluation of Θ and to match the results from the solid model.
2. The proposed beam model, with the appropriate order of expansion, provides better results than those from literature in the twisting angle.
3. The twisting angle behavior along the y-axis (Fig. 6) is not linear, as might be expected from the classical torsion theory; the present model, indeed, takes into account higher-order effects as a result of normal stresses, torsional-bending coupling, and section warping.

Bridge-Like Section

A clamped-clamped, bridge-like cross-section beam is considered. The geometric characteristics have been taken from Gruttmann and Wagner (2001). Fig. 7 shows the geometry of the considered model, and Table 7 presents the dimensions of the beam. Young's modulus, E, is equal to 210 GPa. The Poisson's ratio, ν, is equal to

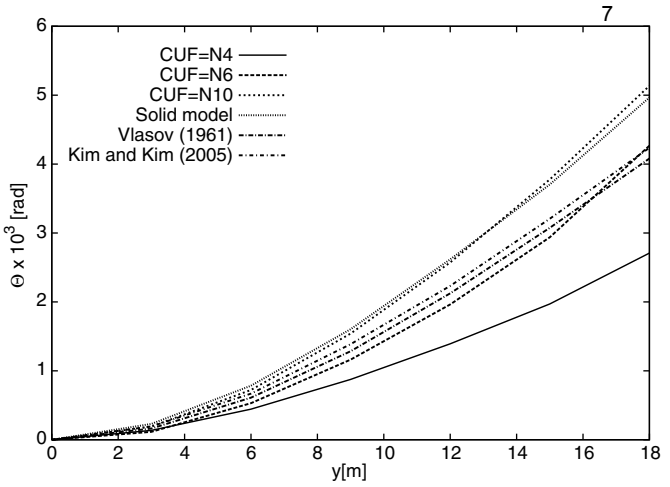

Fig. 6. Twisting angle of the C-shaped cross-section beam along the y-axis; comparisons between different models

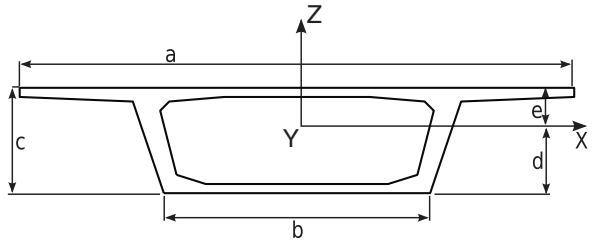

Fig. 7. Bridge-like cross section

Table 7. Bridge-like Cross-Section Dimensions

Dimension	(m)
a	15.200
b	7.300
c	3.450
d	2.155
e	1.295
L	100

0.3. A total of 40 elements B4 are used in the axial discretization. An MSC Nastran model is used for comparison purposes, and solid elements are used.

The bending analysis is first considered. A uniform distributed load, P_S, is applied to the top surface of the cross section. P_S is equal to 10,000 Pa, and Fig. 8(a) shows the bending loading condition. Table 8 shows the maximum values of the vertical displacement for different beam theories. The last row reports the value obtained in MSC Nastran. The total number of degrees of freedom of each model is given in the second column. The position of each indicated displacement value is reported in the last two columns. The deformed structure is shown in Fig. 9. The maximum values of the axial stress, σ_{yy}, at different spanwise locations are presented in Table 9 with an indication of the related cross-section location. Fig. 10 shows the vectorial shear stress distribution over the cross section at $y = L/4$. Different beam theories are considered. A comparison of stress distributions, computed by means of a fourth-order beam model and solid elements, is presented in Fig. 11.

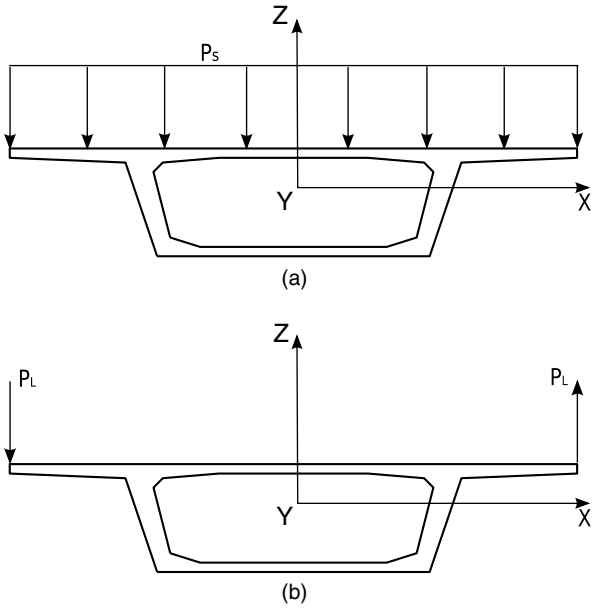

Fig. 8. Loading conditions of the bridge-like structure: (a) bending; (b) torsion

Table 8. Value and Position of the Maximum Vertical Displacement, u_z, for Different Beam Models and Comparison with Solid Elements; Bending Loading

Model	DOFs	$u_z \times 10^1$ (m)	x	z
EBBM	605	−0.989	—[a]	—
TBM	605	−1.010	—	—
1	1,089	−1.010	$-a/2 < x < a/2$	e
2	2,178	−1.000	$-a/2 < x < a/2$	0.994
3	3,630	−1.030	$\pm a/2$	0.994
4	5,445	−1.040	$\pm a/2$	0.994
Solid	351,288	−1.070	$\pm a/2$	0.994

Note: $y = L/2$.
[a]Constant along the section.

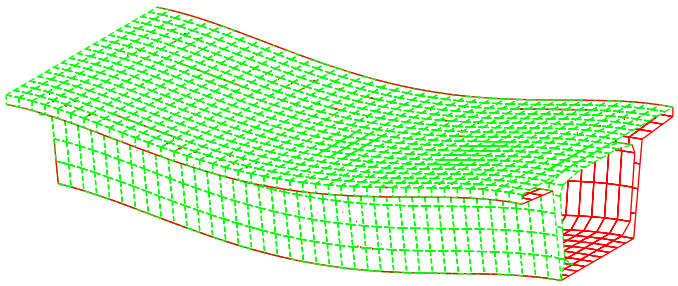

Fig. 9. Deformed bridge-like beam, bending loading; $N = 4$

A torsion analysis is considered as the second assessment of the bridge-like structure. A uniform distributed linear load, P_L, is applied to the top surface edges of the cross section. P_L is equal to 100,000 N/m. Fig. 8(b) shows the torsion loading condition. The maximum displacement values at $y = L/2$ are reported in Table 10. The deformed structure is shown in Fig. 12. Vectorial shear stress distributions at $y = L/4$ are shown in Fig. 13 for differ-ent beam theories. Shear stress distributions, computed by means of

Table 9. Value and Position of Maximum Normal Stress, σ_{yy}, at Different Spanwise Locations; Bending Loading Case

Model	$\sigma_{yy} \times 10^7$ (Pa)	x	z
	$y = L/2$		
EBBM	0.716	$-b/2 < x < b/2$	$-d$
TBM	0.716	$-b/2 < x < b/2$	$-d$
$N = 1$	0.716	$-b/2 < x < b/2$	$-d$
$N = 2$	0.706	$-b/2 < x < b/2$	$-d$
$N = 3$	0.714	$\pm b/2$	$-d$
$N = 4$	0.712	$\pm b/2$	$-d$
	$y = L/4$		
EBBM	0.179	$-b/2 < x < b/2$	$-d$
TBM	0.179	$-b/2 < x < b/2$	$-d$
$N = 1$	0.178	$-b/2 < x < b/2$	$-d$
$N = 2$	0.168	$-b/2 < x < b/2$	$-d$
$N = 3$	0.177	$\pm b/2$	$-d$
$N = 4$	0.176	$\pm b/2$	$-d$
	$y = 0$		
EBBM	−1.432	$-b/2 < x < b/2$	$-d$
TBM	−1.432	$-b/2 < x < b/2$	$-d$
$N = 1$	−1.433	$-b/2 < x < b/2$	$-d$
$N = 2$	−1.681	$-b/2 < x < b/2$	$-d$
$N = 3$	−2.446	$\pm b/2$	$-d$
$N = 4$	−3.067	$\pm b/2$	$-d$

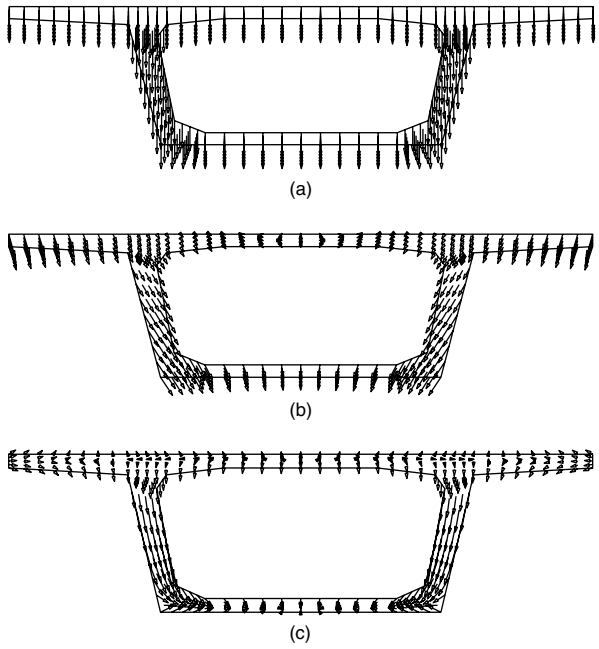

Fig. 10. Vectorial shear stress distribution at $y = L/4$ for different beam theories; bending loading case: (a) $\sigma_{xy} + \sigma_{zy}$, TBM; (b) $\sigma_{xy} + \sigma_{zy}$, $N = 2$; (c) $\sigma_{xy} + \sigma_{zy}$, $N = 4$

a fourth-order beam model and MSC Nastran, are presented in Fig. 14. Fig. 15 shows the comparisons between a fourth-order theory and the solid model in shear stress along some paths obtained on section reported in Figs. 11 and 14. The following comments can be made:

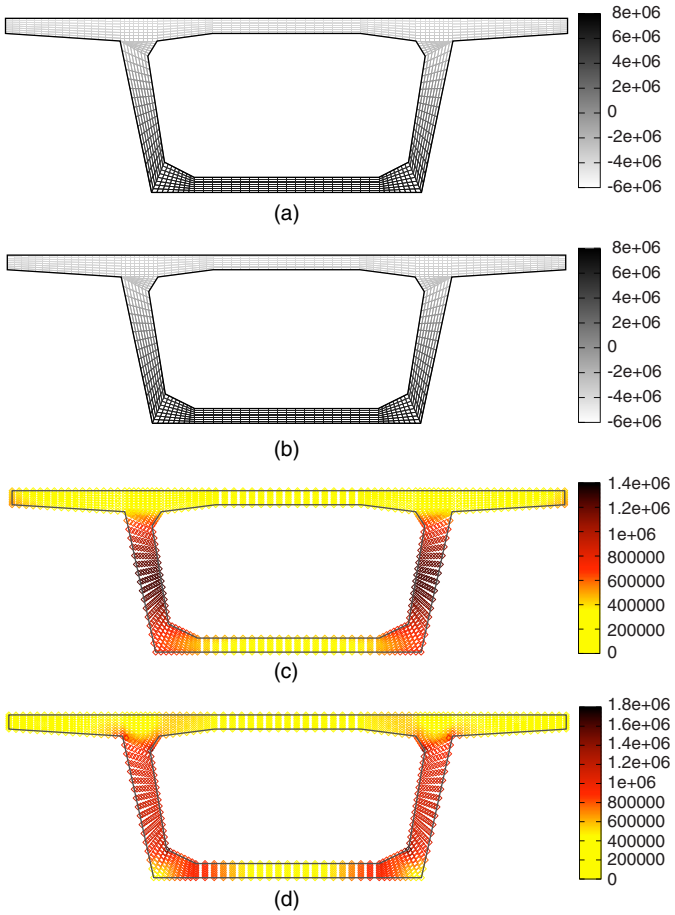

Fig. 11. Comparison of stress-fields (Pa) between the fourth-order beam and solid elements; $y = L/2$: (a) σ_{yy}, $N = 4$; (b) σ_{yy}, solid; (c) $\sigma_{xy} + \sigma_{zy}$, $N = 4$; (d) $\sigma_{xy} + \sigma_{zy}$, solid

Table 10. Value and Position of the Maximum Displacements for Different Beam Theories and Comparison with Solid Elements; Torsion Loading Case

Model	DOFs	$u \times 10^{-3}$ (m)	x	z
		u_x		
EBBM	605	0	—	—
TBM	605	0	—	—
$N = 1$	1,089	+0.270	$-b/2$	$-d$
$N = 2$	2,178	+0.559	$-b/2$	$-d$
$N = 3$	3,630	−0.865	$-a/2$	e
$N = 4$	5,445	−0.906	$-a/2$	e
Solid	351,288	−1.100	$\pm a/2$	0.994
		u_z		
EBBM	605	0	—	—
TBM	605	0	—	—
$N = 1$	1,089	−0.955	$-a/2$	e
$N = 2$	2,178	−2.431	$-a/2$	e
$N = 3$	3,630	−3.176	$-a/2$	e
$N = 4$	5,445	−3.540	$-a/2$	e
Solid	351,288	−5.000	$-a/2$	e

Note: $y = L/2$.

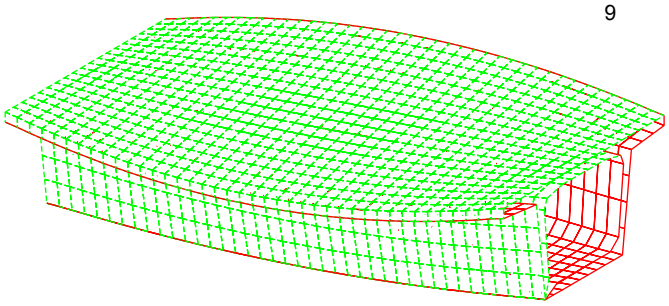

Fig. 12. Deformed bridge-like beam; torsion loading; $N = 4$

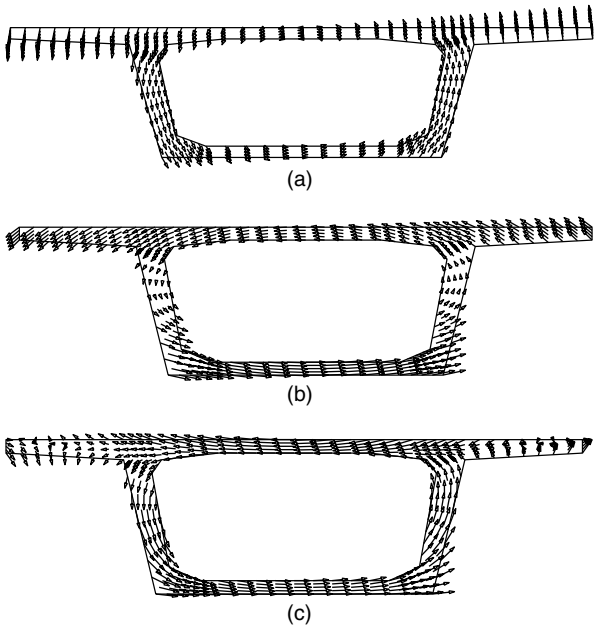

Fig. 13. Vectorial shear stress distribution at $y = L/4$; torsion loading case: (a) $\sigma_{xy} + \sigma_{zy}$, $N = 1$; (b) $\sigma_{xy} + \sigma_{zy}$, $N = 2$; (c) $\sigma_{xy} + \sigma_{zy}$, $N = 4$

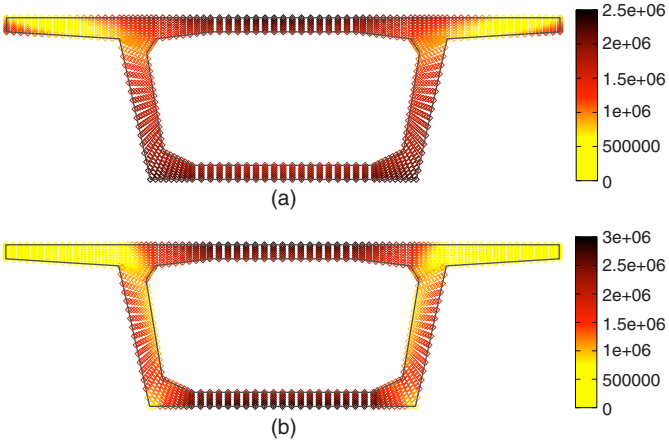

Fig. 14. Comparison of the shear stress field (Pa) between the fourth-order beam and solid elements; $y = L/4$: (a) $\sigma_{xy} + \sigma_{zy}$, $N = 4$; (b) $\sigma_{xy} + \sigma_{zy}$, solid

1. The use of higher-order theories significantly enhances the prediction capability of the 1D beam model. This is true for both displacement and stress-fields.

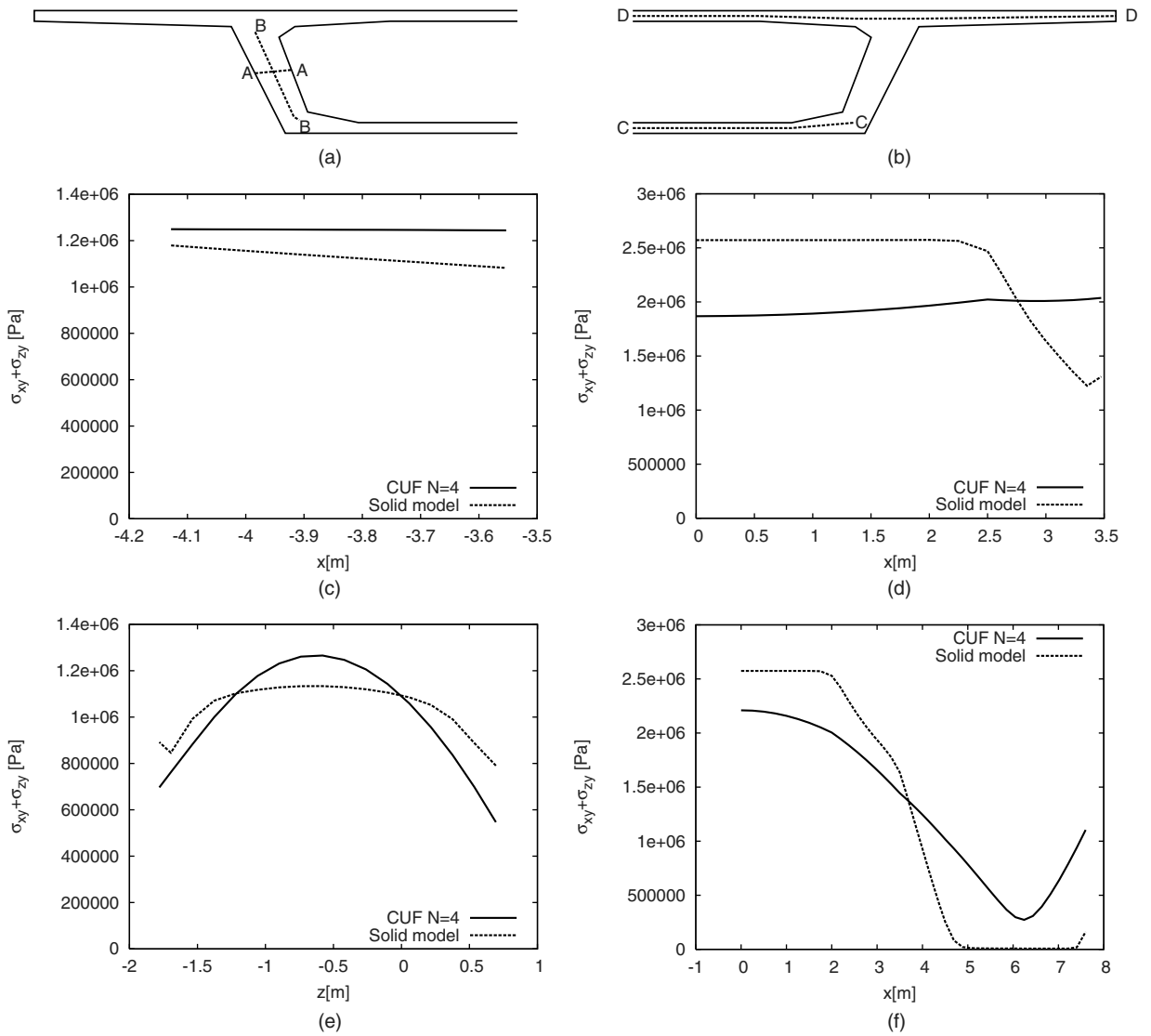

Fig. 15. Behavior of the in-plane shear ($\sigma_{xy} + \sigma_{zy}$) along some sections; comparisons between fourth-order beam model and solid model: (a) sections in bending loading case, $y = L/2$; (b) sections in torsion loading case, $y = L/4$; (c) $\sigma_{xy} + \sigma_{zy}$, section A-A, bending loading case; (d) $\sigma_{xy} + \sigma_{zy}$, section C-C, torsion loading case; (e) $\sigma_{xy} + \sigma_{zy}$, section B-B, bending loading case; (f) $\sigma_{xy} + \sigma_{zy}$, section D-D, torsion loading case

2. As far as the bending analysis is concerned, a third-order beam model is able to detect the right position of the points along the cross section that are affected by the maximum displacement and axial stress values.
3. The use of a fourth-order model permits the establishment of the distribution of stress fields along the cross section, and a significant match is found with the solid element model. The ability of the refined model to respect the boundary value conditions of the shear stress should be pointed out, whereas classical models fail.
4. The torsion analysis has shown an even more important role of higher-order terms than in the bending case. At least a third-order model is needed to detect the right positions of the most deformed and stressed points along the cross section. The use of refined theories appears to be mandatory to furnish significant improvements in the prediction of the torsional structural behavior by means of beam modeling.
5. An $N = 4$ model could fail in detecting the 3D solution in case of torsion. This is a known result from previous CUF works by Carrera et al. (2011), in which up to $N = 11$ were needed to detect the accurate 3D solution in the case of thin-walled structures.
6. The computational costs of the presented beam model are much lower than those necessary for the use of solid elements.

Discussion on Shear Correction Factors for Various Beam Sections

In this paper, shear correction factors are computed for different beam models and cross section geometries. Two different definitions of shear correction factors are used. The first one has been proposed by Cowper (1966), and the second one has been used by Gruttmann and Wagner (2001) and was introduced by Bach and Baumann (1924) and Stojek (1964). Cowper's formulation considers the mean deflection of the cross section, W; the mean angle of rotation of the cross section around the neutral axis, Φ; and the total transverse shear force acting on the cross section, Q, as follows:

$$W = \frac{1}{A} \int \int u_x dx dz \tag{21}$$

$$\Phi = \frac{1}{I}\int\int xu_y dxdz \tag{22}$$

$$Q = \int\int \sigma_{xy} dxdz \tag{23}$$

where A = cross-section area; and I = moment of inertia of the cross section. The shear correction factor, K^C, is computed by exploiting the following equation:

$$\frac{\partial W}{\partial y} + \Phi = \frac{Q}{K^C AG} \tag{24}$$

where G = shear modulus. Subscripts x and z will be used to indicate whether K^C is related to a load acting along the x- or z-direction, respectively. The second method adopted for the computation of the shear correction factor uses the following formula:

$$\int\int (\sigma_{yx}^2 + \sigma_{yz}^2) dxdz = \frac{F_x^2}{K_x^G A} + \frac{F_z^2}{K_z^G A} \tag{25}$$

where the shear correction factors, K_x^G and K_z^G, are computed by letting F_z and F_x be equal to zero, respectively.

A square cross-section clamped beam is first considered. A concentrated force, F_z, is applied at the center point of the free tip. Table 11 shows the shear correction factors for different Poisson's ratio values. A bridge-like cross section is then considered. The geometry of the structure is shown in Fig. 7. The Poisson's ratio, ν, is as high as 0.2. The obtained shear correction factors are reported in Table 12. The following statements hold:

1. The analysis of the square cross section shows excellent agreement with the data retrieved from literature. This represents a further validation of the proposed beam model.
2. A third-order, $N = 3$ beam theory is sufficient to detect the shear correction factors; that is, a cubic beam model is able to obtain the correct shear distribution on a square cross section.
3. The analysis of the bridge-like cross section highlights the improvements obtained by the refined models when computing the shear correction factors; both formulations seem to converge to the results derived by Gruttmann and Wagner (2001).
4. No significant differences were found when the shear correction factor computation approach is changed; that is, both the Cowper and Gruttmann approaches lead to similar values of correction factors.

Table 11. Shear Correction Factors for a Square Cross Section

Model	$\upsilon = 0$	$\upsilon = 0.25$
	K_z^C	
$N = 1$	1.001	1.001
$N = 2$	1.001	1.001
$N = 3$	0.834	0.848
$N = 4$	0.834	0.848
Cowper (1966)	0.833	0.847
	K_z^G	
$N = 1$	1.000	1.000
$N = 2$	1.000	0.987
$N = 3$	0.833	0.829
$N = 4$	0.833	0.829
Gruttmann and Wagner (2001)	0.833	0.830

Table 12. Shear Correction Factors for the Bridge-like Cross Section

Model	K_z	K_x
	K^C	
$N = 1$	1.000	1.000
$N = 2$	0.681	0.961
$N = 3$	0.338	0.707
$N = 4$	0.320	0.689
$N = 5$	0.308	0.625
	K^G	
$N = 1$	1.000	1.000
$N = 2$	0.672	0.963
$N = 3$	0.330	0.699
$N = 4$	0.317	0.681
$N = 5$	0.301	0.619
Gruttmann and Wagner (2001)	0.231	0.599

Conclusions

This work has presented the static analysis of compact and bridge-like structural models by means of refined beam theories. Higher-order models have been obtained by employing the Carrera Unified Formulation, which permits us to deal with any order of beam theories without need of ad hoc implementations. In other words, the order of the theory is considered as an input of the analysis. The finite-element method has been adopted to deal with arbitrary geometries, loadings, and boundary conditions. Compact square cross sections and bridge-like geometries have been considered. Bending and torsion loading conditions have been addressed. Isotropic materials have been used. The obtained results have been compared with those available from literature, with analytical approaches, and with solid finite-element models.

The proposed model appears to be able to consider any deformation/stress state of the considered compact and bridge-like sections, leading to quasi-3D stress states. The adoption of refined theories is mandatory whenever

- The slenderness ratio is not high;
- The cross-section geometry is not compact;
- Torsion behavior has to be investigated;
- End effects caused by boundary conditions have to be studied.

CUF has shown its capacity to deal with each of these issues with acceptable computational efforts.

The use and the definition of shear correction factors appears very much questionable, as has been pointed out by many authors; its definition is a problem-dependent parameter. The adoption of refined theories, in fact, offers a more flexible approach that is independent of the features of the addressed structural problem. This work does not propose new correction factors; the analysis was carried out to underline how the use of higher-order beam models can be a valid alternative to the use of such factors, the definition of which is extremely difficult to assess for general problems. CUF makes this approach particularly attractive because its hierarchical capabilities, together with the possibility of addressing arbitrary geometries, make it easy to obtain results that are usually furnished by more cumbersome 2D or 3D models. Future investigations could be directed towards considering anisotropic and non homogeneous sections and dynamic responses.

Acknowledgments

The financial support from the Regione Piemonte project MICROCOST is gratefully acknowledged.

References

Bach, C., and Baumann, R. (1924). *Elastizität und Festigkeit*, Springer, Berlin.

Back, S. Y., and Will, K. M. (1998). "A shear-flexible element with warping for thin-walled open beams." *Int. J. Numer. Methods Eng.*, 43(7), 1173–1191.

Bathe, K. (1996). *Finite element procedure*, Prentice Hall, Englewood Cliffs, NJ.

Berdichevsky, V. L., Armanios, E., and Badir, A. (1992). "Theory of anisotropic thin-walled closed-cross-section beams." *Compos. Eng.*, 2(5–7), 411–432.

Carrera, E. (1995). "A class of two-dimensional theories for multilayered plates analysis." *Atti Accad. Sci. Torino. Cl. Sci. Fis. Mat. Nat.*, 19(20), 49–87.

Carrera, E. (2002). "Theories and finite elements for multilayered, anisotropic, composite plates and shells." *Arch. Comput. Methods Eng.*, 9(2), 87–140.

Carrera, E. (2003). "Theories and finite elements for multilayered plates and shells: A unified compact formulation with numerical assessment and benchmarking." *Arch. Comput. Methods Eng.*, 10(3), 215–296.

Carrera, E., and Brischetto, S. (2008). "Analysis of thickness locking in classical, refined, and mixed multilayered plate theories." *Compos. Struct.*, 82(4), 549–562.

Carrera, E., and Giunta, G. (2010). "Refined beam theories based on a unified formulation." *Int. J. Appl. Mech. Eng.*, 2(1), 117–143.

Carrera, E., and Petrolo, M. (2011). "On the effectiveness of higher-order terms in refined beam theories." *J. Appl. Mech.*, 78(2).

Carrera, E., and Petrolo, M. (2012). "Refined beam elements with only displacement variables and plate/shell capabilities." *Meccanica*, 47(3), 537–556.

Carrera, E., Brischetto, S., and Robaldo, A. (2008). "Variable kinematic model for the analysis of functionally graded material plates." *AIAA J.*, 46(1), 194–203.

Carrera, E., Giunta, G., Nali, P., and Petrolo, M. (2010a). "Refined beam elements with arbitrary cross-section geometries." *Comput. Struct.*, 88(5–6), 283–293.

Carrera, E., Giunta, G., and Petrolo, M. (2010b). "A modern and compact way to formulate classical and advanced beam theories." Chapter 4, *Developments and applications in computational structures technology*, B. H. V. Topping et al., eds., Saxe-Coburg Publications, Stirlingshire, UK, 75–112.

Carrera, E., Petrolo, M., and Nali, P. (2011). "Unified formulation applied to free vibrations finite element analysis of beams with arbitrary section." *Shock Vib.*, 18(3), 485–502.

Carrera, E., Petrolo, M., and Varello, A. (2012). "Advanced beam formulations for free vibration analysis of conventional and joined wings." *J. Aerosp. Eng.*

Cowper, G. R. (1966). "The shear coefficient in Timoshenko's beam theory." *J. Appl. Mech.*, 33(2), 335–340.

de Saint-Venant, A. (1856). "Mémoire sur la flexion des prismes, sur les glissements transversaux et longitudinaux qui l accompagnent lorsquelle ne sopére pas uniformément ou en arc de cercle, et sur la forme courbe affectée alors par leurs sections transversales primitivement planes." *J. Math. Pures Appl.*, 1 , 8 9 –189 (in French).

Dong, S. B., Kosmatka, J. B., and Lin, H. C. (2001). "On Saint-Venant's problem for an inhomogeneous, anisotropic cylinder—Part I: Methodology for Saint-Venant solutions." *J. Appl. Mech.*, 68(3), 376–381.

El Fatmi, R. (2007a). "Nonuniform warping including the effects of torsion and shear forces. Part I: A general beam theory." *Int. J. Solids Struct.*, 44(18–19), 5912–5929.

El Fatmi, R. (2007b). "Nonuniform warping including the effects of torsion and shear forces. Part II: Analytical and numerical applications." *Int. J. Solids Struct.*, 44(18–19), 5930–5952.

El Fatmi, R. (2007c). "A nonuniform warping theory for beams." *C.R. Mec.*, 335(8), 467–474.

Euler, L. (1744). *De curvis elasticis*." *Methodus inveniendi lineas curvas maximi minimive proprietate gaudentes, sive solutio problematis isoperimetrici lattissimo sensu accepti*, Bousquet, Geneva.

Ghazouani, N., and El Fatmi, R. (2010). "Higher order composite

Yu, W., and Hodges, D. H. (2004). "Elasticity solutions versus asymptotic sectional analysis of homogeneous, isotropic, prismatic beams."

Gruttmann, F., and Wagner, W. (2001). "Shear correction factors in Timoshenko's beam theory for arbitrary shaped cross-sections." *Comput. Mech.*, 27(3), 199–207.

Gruttmann, F., Sauer, R., and Wagner, W. (1999). "Shear stresses in prismatic beams with arbitrary cross-sections." *Int. J. Numer. Methods Eng.*, 45(7), 865–889.

Ieşan, D. (1986). "On Saint-Venant's problem." *Arch. Ration. Mech. Anal.*, 91(4), 363–373.

Kanok-Nukulchai, W., and Shik Shin, Y. (1984). "Versatile and improved higher-order beam elements." *J. Struct. Eng.*, 110(9), 2234–2249.

Kapania, K., and Raciti, S. (1989). "Recent advances in analysis of laminated beams and plates, part I: Shear effects and buckling." *AIAA J.*, 27(7), 923–935.

Kim, N. I., and Kim, M. Y. (2005). "Exact dynamic/static stiffness matrices of nonsymmetric thin-walled beams considering coupled shear deformation effects." *Thin-Walled Struct.*, 4 3 (5) , 701–734.

Krayterman, B. L., and Krayterman, A. B. (1987). "Generalized nonuniform torsion of beams and frames." *J. Struct. Eng.*, 113(8), 1772–1787.

Krishna Murty, A. V. (1985). "On the shear deformation theory for dynamic analysis of beams." *J. Sound Vib.*, 101(1), 1–12.

Ladéveze, P., and Simmonds, J. (1998). "New concepts for linear beam theory with arbitrary geometry and loading." *Eur. J. Mech., A: Solids*, 17(3), 377–402.

Librescu, L., and Song, O. (1992). "On the static aeroelastic tailoring of composite aircraft swept wings modeled as thin-walled beam structures." *Compos. Eng.*, 2(5–7), 497–512.

Mechab, I., Tounsi, A., Benatta, M. A., and Bedia, E. A. (2008). "Deformation of short composite beam using refined theories." *J. Math. Anal. Appl.*, 346(2), 468–479.

Mucichescu, D. T. (1984). "Bounds for stiffness of prismatic beams." *J. Struct. Eng.*, 110(6), 1410–1414.

Novozhilov, V. V. (1961). *Theory of elasticity*, Pergamon, Oxford, UK.

Pai, P. F., and Schulz, M. J. (1999). "Shear correction factors and an energy-consistent beam theory." *Int. J. Solids Struct.*, 36(10), 1523–1540.

Qin, Z., and Librescu, L. (2002). "On a shear-deformable theory of anisotropic thin-walled beams: Further contribution and validations." *Compos. Struct.*, 56(4), 345–358.

Reddy, J. N. (2004). *Mechanics of laminated composite plates and shells. Theory and Analysis*, 2nd Ed., CRC Press, Boca Raton, FL. Schardt, R. (1966). "Eine erweiterung der technischen biegetheorie zur berechnung prismatischer faltwerke." *Der Stahlbau*, 35, 161–171 (in German).

Schardt, R. (1989). *Verallgemeinerte technische biegetheorie*, Springer Verlag, Darmstadt, Germany (in German).

Silvestre, N. (2007). "Generalized beam theory to analyze the buckling behavior of circular cylindrical shells and tubes." *Thin-Walled Struct.*, 45(2), 185–198.

Silvestre, N., and Camotim, D. (2002). "First-order generalized beam theory for arbitrary orthotropic materials." *Thin-Walled Struct.*, 40(9), 791–820.

Sokolnikoff, I. S. (1956). *Mathematical theory of elasticity*, McGraw-Hill, New York.

Stojek, D. (1964). "Zur schubverformung in biegebalken." *ZAMM*, 44(8–9), 393–396 (in German).

Timoshenko, S. P. (1921). "On the correction for shear of the differential equation for transverse vibrations of prismatic bars." *Philosophical Magazine*, 41, 744–746.

Timoshenko, S. P., and Goodier, J. N. (1970). *Theory of elasticity*, McGraw-Hill, New York.

Tralli, A. (1986). "A simple hybrid model for torsion and flexure of thin-walled beams." *Comput. Struct.*, 22(4), 649–658.

Tsai, S. W. (1988). *Composites design*, 4th Ed., Think Composites, Dayton, OH.

Vlasov, V. Z. (1961). *Thin-walled elastic beams*, Israel Program for Scientific Transaction, Jerusalem, Israel.

Volovoi, V. V., and Hodges, D. H. (2000). "Theory of anisotropic thin-walled beams." *J. Appl. Mech.*, 67(3), 453–459.

Wagner, W., and Gruttmann, F. (2002). "A displacement method for the analysis of flexural shear stresses in thin-walled isotropic composite beams." *Comput. Struct.*, 80(24), 1843–1851.

Washizu, K. (1968). *Variational methods in elasticity and plasticity*, Pergamon, Oxford, UK.

Yu, W., and Hodges, D. H. (2004). "Elasticity solutions versus asymptotic sectional analysis of homogeneous, isotropic, prismatic beams." *J. Appl. Mech.*, 71(1), 15–23.

Yu, W., Volovoi, V. V., Hodges, D. H., and Hong, X. (2002). "Validation of the variational asymptotic beam sectional analysis (VABS)." *AIAA J.*, 40(10), 2105–2113.